

STG: Spatiotemporal Graph Neural Network with Fusion and Spatiotemporal Decoupling Learning for Prognostic Prediction of Colorectal Cancer Liver Metastasis

Yiran Zhu[†]

School of Computer Science and
Technology
University of Chinese Academy of
Sciences
Beijing, China
ciaran_study@yeah.net

Wei Yang[†]

School of Computer Science and
Technology
University of Chinese Academy of
Sciences
Beijing, China
sheepwei_2023@qq.com

Yan su

School of Computer Science and
Technology
University of Chinese Academy of
Sciences
Beijing, China
1227698971@qq.com

Zesheng Li

School of Computer Science and
Technology
University of Chinese Academy of
Sciences
Beijing, China
2022111515@stu.sufe.edu.cn

Chengchang Pan*

School of Computer Science and
Technology
University of Chinese Academy of
Sciences
Beijing, China
chpan.infante@qq.com

Honggang Qi*

School of Computer Science and
Technology
University of Chinese Academy of
Sciences
Beijing, China
hgqi@ucas.ac.cn

ABSTRACT

We propose a multimodal spatiotemporal graph neural network (STG) framework to predict colorectal cancer liver metastasis (CRLM) progression. Current clinical models do not effectively integrate the tumor's spatial heterogeneity, dynamic evolution, and complex multimodal data relationships, limiting their predictive accuracy. Our STG framework combines preoperative CT imaging and clinical data into a heterogeneous graph structure, enabling joint modeling of tumor distribution and temporal evolution through spatial topology and cross-modal edges. The framework uses GraphSAGE to aggregate spatiotemporal neighborhood information and leverages supervised and contrastive learning strategies to enhance the model's ability to capture temporal features and improve robustness. A lightweight version of the model reduces parameter count by 78.55%, maintaining near-state-of-the-art performance. The model jointly optimizes recurrence risk regression and survival analysis tasks, with contrastive loss improving feature representational discriminability and cross-modal consistency. Experimental results on the MSKCC CRLM dataset show a time-adjacent

*corresponding author

[†]Co-first author

Permission to make digital or hard copies of part or all of this work for personal or classroom use is granted without fee provided that copies are not made or distributed for profit or commercial advantage and that copies bear this notice and the full citation on the first page. Copyrights for third-party components of this work must be honored. For all other uses, contact the owner/author(s).

WOODSTOCK '18, June, 2018, El Paso, Texas USA

© 2018 Copyright held by the owner/author(s). 978-1-4503-0000-0/18/06...\$15.00
<https://doi.org/10.1145/1234567890>

accuracy of 85% and a mean absolute error of 1.1005, significantly outperforming existing methods. The innovative heterogeneous graph construction and spatiotemporal decoupling mechanism effectively uncover the associations between dynamic tumor microenvironment changes and prognosis, providing reliable quantitative support for personalized treatment decisions.

CCS CONCEPTS

- Applied computing → Life and medical sciences; Health informatics.

KEYWORDS

Spatiotemporal Graph Neural Networks, Multimodal Fusion, Colorectal Cancer Liver Metastasis Prognosis, Prognostic Prediction

ACM Reference format:

Anonymous Author(s). 2025. STG : Spatiotemporal Graph Neural Network with Fusion and Spatiotemporal Decoupling Learning for Prognostic Prediction of Colorectal Cancer Liver Metastasis. In *Proceedings of ACM Woodstock conference (WOODSTOCK'25)*. ACM, New York, NY, USA, 9 pages. <https://doi.org/XXXXXXX.XXXXXXX>

1 Introduction

Colorectal cancer is one of the most prevalent malignant tumors globally, with approximately half of patients developing liver metastasis during the course of the disease, often indicating a

significant worsening of prognosis [1, 2]. Although liver resection combined with systemic therapy can result in a 5-year survival rate exceeding 50% for some CRLM patients, the majority still experience tumor recurrence postoperatively, leading to a low long-term survival rate [1]. Accurately predicting which patients are more likely to experience recurrence or have a shorter survival time before surgery is of critical clinical importance for formulating personalized treatment plans (e.g., selecting more aggressive adjuvant therapies or forgoing high-risk surgeries). However, traditional prognostic assessments primarily rely on clinical experience and risk scores (e.g., based on the number, size, and CEA levels of metastases), which are subjective and fail to fully utilize the rich information provided by imaging and other data, leading to limited predictive accuracy. Over the past decades, many prognostic models for CRLM have been developed using both clinical and imaging features [3], yet their performance and validation vary widely. Therefore, quantifying tumor spatiotemporal evolution features precisely and achieving personalized prognostic prediction has become a pressing challenge in clinical decision-making.

Recent advances in deep learning for medical image analysis have opened new possibilities for prognostic prediction. Several studies have trained convolutional neural networks on imaging data to automatically extract features for survival prediction or recurrence risk assessment [4]. Unlike traditional handcrafted features (radiomics), deep learning uncovers higher-dimensional image representations and has shown superior performance in tumor prognosis. However, relying on a single modality, such as imaging or clinical data alone, often fails to capture the full biological behavior of tumors. Unimodal models still have limitations in accuracy and robustness. To improve prognostic predictions, multimodal data fusion methods have emerged. By integrating imaging, clinical indicators, pathology, and molecular data, these approaches better reflect tumor characteristics, enhancing prediction performance [5]. Previous work has shown that multimodal fusion models outperform unimodal ones in tasks like breast cancer screening [6] and predicting responses to neoadjuvant therapy [7]. Furthermore, deep learning models that combine pathology images and genomic data have demonstrated improved prognostic accuracy over traditional risk factors [8]. However, multimodal data present challenges, such as large modality differences and incomplete data. Simple concatenation often ignores the relationships between modalities and underutilizes complementary information, limiting model generalization.

The spatiotemporal evolution of tumors is also crucial for prognosis. Dynamic information, such as changes in tumor burden and lesion growth patterns over time, provides key survival indicators. Traditional models primarily use preoperative static data, neglecting disease progression. Incorporating temporal data into modeling can capture variations in tumor progression and improve predictions. However, integrating spatial structure and temporal evolution in deep learning models remains a challenge. A few studies have tried to include temporal imaging data, such as comparing preoperative and postoperative “dynamic radiomics”

features to predict treatment response [9]. Jin et al. developed a multi-task deep learning model using serial imaging that successfully predicted treatment response [10], highlighting the value of longitudinal data. However, designing spatiotemporal fusion models for prognostic analysis is still under exploration.

To address these challenges, this paper proposes a multimodal spatiotemporal prognostic prediction model based on graph neural networks (GNNs) [11] for recurrence and survival prediction in colorectal cancer liver metastasis (CRLM) patients. We construct a spatiotemporal graph using imaging and clinical data to capture tumor spatial features and their evolution over time, efficiently fusing multimodal information through graph neural networks.

Compared to existing methods, our main contributions can be summarized as follows:

- We propose a structured graph representation integrating tumor lesions (CT imaging features) and clinical variables, where spatial topology edges model tumor microenvironments and cross-modal edges capture image-clinical interactions. This eliminates heuristic feature concatenation and provides an interpretable paradigm for multimodal fusion.
- To address temporal granularity and small-sample robustness, we design a dynamic graph reconstruction framework based on GraphSAGE. By jointly optimizing supervised and contrastive objectives, it learns fine-grained spatiotemporal patterns of tumor evolution while reducing overfitting risks.
- We decouple spatial and temporal learning via a parameter-efficient architecture: GraphSAGE for topology aggregation and LSTM for progression dynamics. This achieves 78.5% parameter reduction with competitive accuracy, enabling practical deployment.

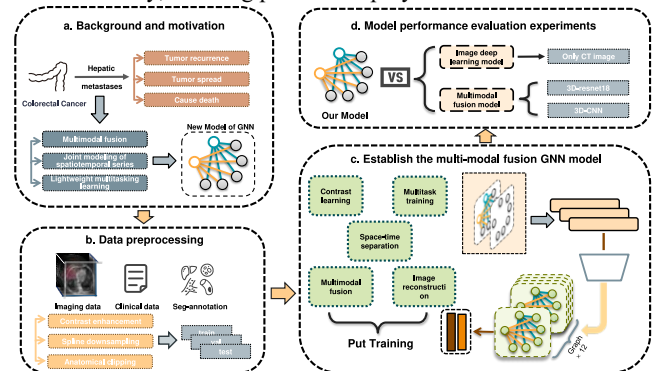


Figure 1: This is a rough flow chart of our experiment.

2 Related Work

In colorectal cancer liver metastasis (CRLM) prognostic research, traditional unimodal models have long been limited. Early studies mainly relied on clinical scoring systems and statistical methods based on image features. For example, Cox regression models often focus on single clinical variables [12], overlooking the spatiotemporal evolution of tumors and the complexity of

multimodal data such as imaging. Unimodal deep learning models based on imaging can capture tumor spatial heterogeneity but struggle to integrate clinical information. Liu et al. proposed a 3D ResNet model that extracts tumor features from preoperative CT imaging to predict survival risk [13], but its performance is constrained by the static nature of imaging, which cannot capture the dynamic evolution of the tumor microenvironment. Similarly, the nomogram scoring system developed by Fong et al. predicts recurrence risk using clinical indicators like CEA levels and metastasis count [14], but its linear assumptions fail to capture the complex nonlinear relationships in clinical data. These limitations of unimodal approaches emphasize the need for integrating spatiotemporal features and multimodal data.

Combining multiple data sources has proven effective in enhancing prediction performance. Early studies combined radiomics with clinical factors to build prognostic models. For example, Kickingereeder et al. showed that integrating imaging features with clinical and genetic data improved survival prediction in glioma [4]. With deep learning advancements, multimodal models have gained attention. McKinney et al. demonstrated that combining multi-view imaging and clinical data improves breast cancer detection accuracy [6], and Zhou et al. proposed a deep model integrating CT imaging and treatment information to predict prognosis for metastatic colorectal cancer patients undergoing bevacizumab treatment [7]. These studies suggest multimodal learning’s potential for medical prognosis. However, current models face challenges in handling modality absence and modeling cross-modal associations, limiting their ability to fully exploit multimodal data [7]. This study seeks to improve multimodal fusion by naturally representing the relationships between imaging regions and clinical variables through graph structures and alignment strategies to address distribution differences between modalities.

Graph neural networks (GNNs), known for handling non-Euclidean structured data, have recently been applied in the medical field to model complex relationships. Fu et al. proposed a multimodal graph network combining cell phenotype distributions from multiplexed imaging with clinical variables, improving breast cancer survival prediction [15]. Wang et al. designed a dual-stream GNN that models and interacts with pathology images and genetic data to predict cancer patient survival [16]. Additionally, Yang et al. integrated molecular and clinical similarity networks into a multi-view graph and used graph convolutional networks (GCN) to extract comprehensive features for prognostic prediction [17]. These studies highlight GNNs’ potential in extracting high-order relational features for survival analysis. However, existing methods focus mainly on static data or single time points, neglecting the temporal dynamics of tumor progression. In this study, we extend GNNs to the spatiotemporal dimension, modeling different tumor regions and their temporal evolution for improved survival prediction.

Combining spatial relationships and temporal information has gained attention in recent machine learning research. In computer vision, Yan et al. introduced a spatiotemporal graph convolutional network (ST-GCN), which uses graph convolutions for spatial

relationships and temporal convolutions to capture dynamic action sequences, excelling in action recognition tasks [18]. In medicine, temporal information integration has been explored, such as the “dynamic radiomics” method, which compares imaging features from different time points to improve treatment response prediction [9]. However, tumor growth and evolution follow complex patterns, and associations between features at different time points are challenging to capture with simple sequential models. Our method, inspired by ST-GCN, adds temporal edges to the graph structure, enabling the model to learn spatial interactions and temporal changes, improving survival outcome predictions.

To fully utilize multimodal data, recent studies have focused on aligning feature distributions across modalities while preserving modality-specific information. Hao et al. proposed a cross-modal alignment network that separately encodes pathology images and genetic data, applying contrastive and discrepancy constraints before fusion to prevent one modality from overwhelming the other, thus improving survival prediction [19]. Multi-task learning is also commonly used to enhance discriminative representations by learning multiple related objectives simultaneously. In prognostic analysis, combining tumor recurrence classification with survival time prediction helps the model understand the impact of tumor invasiveness on both indicators. In this study, we use multi-task training, applying contrastive losses to align imaging and clinical nodes in a shared space while preserving modality-specific features. We also jointly optimize recurrence and survival tasks, enabling the model to handle both classification and regression objectives based on shared graph representations, improving its ability to capture prognostic risks.

3 Methods

The overall architecture of the proposed model is shown in Figure 2, which consists of modules for graph structure construction, spatiotemporal graph reconstruction, and spatiotemporal separation feature extraction. The design of each module is explained in the following sections.

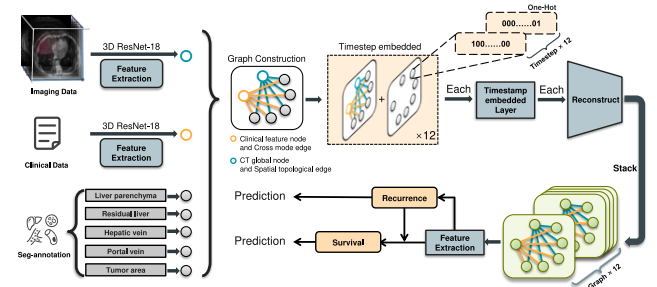


Figure 2: Prognostic model of liver metastases in colorectal cancer using spatio-temporal graph neural network based on fusion and spatio-temporal separation decoupling learning.

3.1 Graph Structure Construction

Based on the multimodal data of each colorectal cancer liver metastasis (CRLM) patient, this study constructs a heterogeneous graph model that integrates anatomical structures and clinical features. The model is realized through the following steps:

In imaging processing, five key anatomical labels are extracted from preoperative contrast-enhanced CT segmentation as image nodes: liver parenchyma, postoperative residual liver, hepatic veins, portal veins, and tumor regions. Features for each anatomical node are first extracted using a pre-trained 3D ResNet-18 model on 3D imaging data. These features are then fused through multi-scale adaptive pooling (with sizes $1 \times 1 \times 1$, $2 \times 2 \times 2$, and $4 \times 4 \times 4$) to combine local details with global context, resulting in a 4096-dimensional feature vector. The entire liver CT volume is input into another 3D ResNet-18 model (adjusted to single-channel input), extracting global image features as a CT global node representing the overall liver anatomy. In clinical processing, clinical indicators (such as age, CEA levels, number of metastases) are standardized and mapped into a 4096-dimensional vector through a fully connected layer to form a clinical feature node, consolidating patient biological data for cross-modal interactions.

Node connections follow spatial topology and semantic rules. In the spatial dimension, the CT global node connects to all five anatomical nodes, with edge attributes defined as normalized spatial centroid coordinates, encoding the spatial relationship between lesions and liver structure. In the cross-modal dimension, the clinical feature node connects to all anatomical nodes, with edge attributes fixed as the vector $[1.0, 0.0, 0.0]$, representing the global impact of clinical data on the tumor microenvironment, minimizing redundant parameters. To distinguish node types, anatomical nodes are labeled as type 0, the CT global node as type 1, and the clinical feature node as type 2. Each patient's data is represented as a heterogeneous graph with 7 nodes (5 anatomical, 1 CT, 1 clinical). This design reduces computational complexity compared to traditional lesion-level graph methods by fixing node types and connections while leveraging multi-scale fusion to balance model efficiency and spatial heterogeneity accuracy.

3.2 Spatiotemporal Graph Reconstruction Framework

To model a patient's dynamic prognosis over time, this study proposes a spatiotemporal graph reconstruction framework based on GraphSAGE. Using GraphSAGE, we extract high-level feature representations from the spatiotemporal graph nodes [20]. As shown in Table 1, this framework extends the preoperative heterogeneous graph over time and combines graph convolution with recurrent neural networks (RNNs) to fuse multimodal spatiotemporal features. The process is as follows:

Temporal Graph Reconstruction. The model is based on the preoperative static heterogeneous graph and simulates the disease progression over a 12-year period post-surgery. For each time step $t \in \{0, 1, \dots, 11\}$, the discrete timestamps are first mapped into 12-dimensional encoding vectors e_t using the embedding layer (1). Then, the time encoding is integrated into the node features via concatenation (2), forming the spatiotemporal enhanced features.

$$e_t = \text{Embedding}(t) \in R^{12} \quad (1)$$

$$\tilde{h}_i^{(t)} = \text{Concat}(h_i, e_t) \quad (2)$$

where $h_i \in R^{d_{in}}$ represents the original node features.

Subsequently, a three-layer GraphSAGE convolution is applied for feature propagation.

$$h_i^{(t,l+1)} = \text{GraphSAGE}\left(\tilde{h}_i^{(t,l)}, N(v_i)\right) \quad (3)$$

The key design lies in independently reconstructing the graph structure from the preoperative original features at each time step (rather than relying on the state from the previous time step), which helps avoid error propagation across time steps. At each time step, three layers of GraphSAGE convolution are used to aggregate information from neighboring nodes (3), generating node embeddings $h_i^{(t)}$ for each time step. This process ultimately forms a temporal graph sequence consisting of 12 time steps, which comprehensively characterizes the potential state evolution of the disease over each postoperative year.

Table 1: Space-time map reconstruction pseudo-code.

Temporal Graph Reconstruction	
Input: Graph $G(V, E)$, time steps T , node features $X \in R^{ V \times d}$	
Output: Temporal embeddings $H \in R^{ V \times h}$	
1: procedure TEMPORAL-RECONSTRUCTION(G, T, X)	
2: Initialize time_encoder: $E_t \leftarrow \text{Embedding}(T, T)$	
3: $H_temp \leftarrow []$ # Temporal feature container	
4: for $t \in [0, T-1]$ do	
5:	$\tau \leftarrow E_t(\text{torch.full}(V , t))$ # Time encoding
6:	$X_t \leftarrow \text{CONCAT}(X, \tau)$ # $[V , d+T]$
7:	$H_t \leftarrow \text{GraphSAGE}(X_t, E)$ # Spatial aggregation
8:	$H_temp.append(H_t)$
9:	$H_seq \leftarrow \text{stack}(H_temp)$ # $[T, V , h]$
10: return H_seq	

Spatiotemporal Feature Aggregation. To model the hierarchical interactions in the reconstructed graph, we first flatten the temporal graph sequence by concatenating node features across all time steps into a unified graph. This allows joint modeling of spatiotemporal dependencies through spatial edges preserved from the original topology.

The unified graph is then processed by a two-layer GraphSAGE module with mean aggregation. The first layer aggregates immediate neighborhood features (e.g., tumor-clinical relationships), while the second layer captures higher-order structural patterns (e.g., multi-hop anatomical dependencies). Formally, for node v_i :

$$h_i^{(l)} = \sigma\left(W_l \times \text{MEAN}\left(h_i^{(l-1)}, \{h_j^{(l-1)}\}_{j \in N(i)}\right)\right), l = 1, 2 \quad (4)$$

where W_l are learnable parameters and σ denotes the ReLU activation.

Finally, we apply global average pooling over all nodes to obtain the graph-level representation h_{graph} , which is fed into a linear layer for prognosis prediction. This design ensures parameter efficiency while maintaining discriminative spatiotemporal patterns.

Multi-task Learning Structure. The model uses a dual-branch structure to optimize recurrence time regression and survival risk analysis. The recurrence branch maps fused features to continuous postoperative recurrence times, using a mean squared error loss to ensure accuracy. The survival branch, based on the Cox model, improves survival time prediction by optimizing risk score ranking consistency. Both tasks share the spatiotemporal graph representation, with a dynamic weighting strategy to balance objectives: initially, more weight is given to recurrence prediction, focusing on time regression, while the weight for survival analysis increases over time to guide multi-objective optimization. This strategy helps prevent early overfitting, improving generalization.

Supervised Learning - Contrastive Learning Joint Training. Experiments show that directly using the temporal graph reconstruction method still limits the model's performance. We believe this phenomenon arises because, during the temporal graph reconstruction phase, no explicit training strategy is set to regulate the quality of the reconstructed graph. Therefore, we introduce contrastive learning, jointly training it with supervised learning, which significantly improves the spatiotemporal graph reconstruction quality and the model's prediction performance.

This strategy ensures stable predictions in complex clinical scenarios by constraining feature space consistency. Before training, data augmentation is applied to the input heterogeneous graphs: (1) Random node masking — anatomical nodes are removed with a 5% probability to simulate missing features in clinical data; (2) Feature perturbation — Gaussian noise (std = 0.1) is added to retained node features to simulate errors in image segmentation or clinical measurements. The augmented sample pairs (original and augmented graphs) are encoded to generate fused features, with feature similarity constrained using contrastive loss. This forces the model to map augmented views of the same patient to nearby regions in feature space, while separating features of different patients. This improves robustness to missing data and noise, with results showing over 85% prediction stability even with 20% node missing.

Loss Function Design. To comprehensively guide model optimization, this study integrates four types of loss components: recurrence regression loss, survival analysis loss, contrastive learning loss, and temporal consistency loss, forming a multi-objective joint optimization framework.

$$L_{time} = \frac{1}{N-1} \sum_{t=1}^{N-1} ReLU(h_{graph}^{(t)} - h_{graph}^{(t+1)}) \quad (5)$$

The recurrence regression loss (L_{recur}) and survival analysis loss (L_{surv}) are computed using the MSE between the true and predicted times. The contrastive learning loss (L_{cont}) utilizes cosine similarity to align feature representations of augmented

views for the same patient, thereby enhancing the model's robustness to noise and ensuring consistency across modalities. The temporal consistency loss(5) penalizes abrupt changes, using ReLU to enforce positive differences and ensuring smooth transitions between graph-level features across consecutive time steps. Total Loss(6) Function is dynamically weighted to balance the multi-objective optimization:

$$L = \alpha L_{recur} + \beta L_{surv} + \gamma L_{cont} + \delta L_{time} \quad (6)$$

where $\alpha, \beta, \gamma, \delta$ are the weights assigned to each of the individual losses, and the total loss function is used to guide the optimization of the model.

3.3 Spatiotemporal Separation Feature Extraction

In response to the clinical demand for lightweight models, this study proposes a decoupled spatiotemporal modeling framework that achieves efficient feature extraction through independent spatial topology modeling and temporal dynamic capturing mechanisms. This module consists of three parts: the temporal LSTM network, spatial GraphSAGE network, and cascade regression head, significantly reducing computational complexity while ensuring prediction accuracy.

Temporal Feature Extraction leverages the inherent adaptability of LSTM networks to long-span clinical follow-up data. The model feeds the sequence of GraphSAGE node embeddings at each time step into a bidirectional LSTM, capturing dependencies across time steps through the iteration of hidden states. To address the temporal sparsity of yearly follow-up data, the model employs a mean pooling strategy instead of relying solely on the final state, effectively aggregating global temporal patterns. This design avoids the strong assumptions made by traditional RNNs about continuous time steps and is better suited to the non-uniform time intervals characteristic of clinical prognosis predictions.

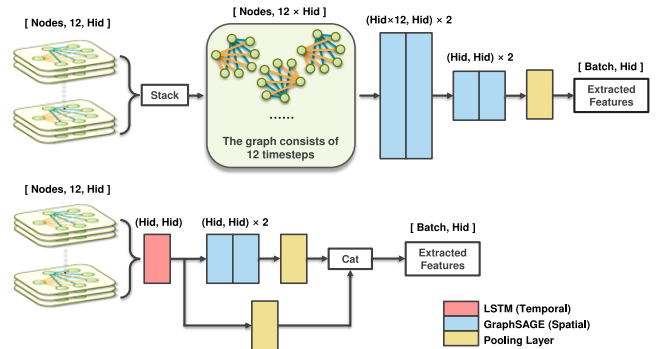


Figure 3: Spatiotemporal Separation Feature Extraction.

Spatial Feature Extraction uses GraphSAGE to model multimodal topological relationships. The spatiotemporal separation mechanism applies spatial graph convolution only to static anatomical structures, with two layers of GraphSAGE aggregating features from neighboring anatomical and clinical nodes. Each layer uses a mean pooling aggregation strategy and PyG's `global_mean_pool` function to convert node-level spatial

embeddings into graph-level representations. This process preserves tumor lesion spatial heterogeneity while avoiding the computational overhead of dynamic graph construction by maintaining a fixed graph structure.

Feature Fusion and Regression Head adopts a cascading design to balance modality specificity and information interaction. After spatial and temporal features are compressed into graph-level vectors through global average pooling, they are concatenated along the feature dimension, forming a joint representation (combined). The regression head uses a minimalist architecture: the recurrence prediction branch is a single-layer linear projection, while the survival prediction branch performs regression after concatenating the recurrence prediction values. Despite sacrificing deep non-linear transformations, experiments show that this lightweight design retains discriminative power in high-dimensional feature spaces, with the final parameter count being only 21.45% of the full model's parameters.

4 Experiments

This section validates the effectiveness of the proposed multimodal spatiotemporal graph neural network (STG) in CRLM prognostic prediction through three aspects: multimodal spatiotemporal modeling, key module contribution, and lightweight deployment feasibility.

4.1 Datasets and Data Preprocessing

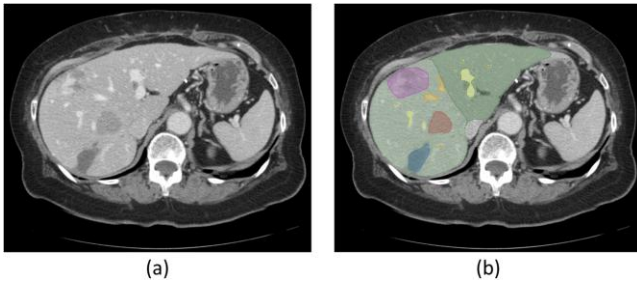


Figure 4: (a) CT volume slices. (b) Segmentation of the liver (green), residual liver (dark green), hepatic veins and portal veins (orange and yellow), and tumors (red, blue, purple).

Datasets. We validated the proposed method using the publicly available CRLM prognostic dataset from the Memorial Sloan Kettering Cancer Center (MSKCC) [21]. This dataset includes preoperative multimodal data from 197 CRLM patients who underwent liver metastasis resection, making it one of the largest and most annotated CRLM prognostic resources. Each patient provides preoperative contrast-enhanced CT images (DICOM format) from the portal venous phase, covering the entire liver in 3D (resolution 512×512). The dataset also includes segmentation of regions of interest (ROIs) by professional radiologists, covering the liver, postoperative residual liver, major blood vessels, and metastatic tumor lesions. Clinical data includes patient demographics (age, sex), pathological TNM staging, number and

distribution of liver metastases, preoperative serum CEA tumor marker levels, and treatment regimens (e.g., neoadjuvant chemotherapy). Postoperative follow-up data includes recurrence events and survival time or status at the last follow-up.

Data Preprocessing. We split the dataset into training, validation, and test sets in a 6:2:2 ratio, ensuring consistent distribution of outcomes like recurrence and death across subsets. During image preprocessing, dynamic histogram equalization enhanced the contrast between the tumor and liver parenchyma, improving lesion boundary visibility. Cubic spline interpolation was used to downsample the CT volume data to a standard resolution of 128×128 , reducing computational complexity. A dynamic cropping strategy based on anatomical landmarks centered at the hepatic portal bifurcation was used to extract 40 slices from the key region. For cases with fewer slices, symmetric padding with -1024 HU was applied to maintain consistency in the 3D convolution network input. Segmentation masks underwent morphological closing ($3 \times 3 \times 3$ kernel) to smooth jagged edges and improve label accuracy. In clinical data preprocessing, time-related variables were standardized to years and normalized using min-max scaling to reduce dimensional differences during model training.

Data Augmentation. To expand the diversity and robustness of training data, we applied two augmentation strategies to increase the dataset size to five times its original scale: (1) Random anatomical node dropout (5% probability) to mimic incomplete clinical feature acquisition; (2) Controlled Gaussian noise injection ($\sigma=0.1$) into node features to replicate segmentation inaccuracies and measurement variability. This fivefold augmentation was applied dynamically during model training.

4.2 Experimental Setup and Evaluation Metrics

Experimental Setup. To ensure fairness and reproducibility, all experiments were conducted in a uniform software and hardware environment. The specific configuration is as follows: the device used was an NVIDIA RTX 4090 GPU (24GB VRAM), and the batch size was set to 64. The AdamW optimizer was chosen with an initial learning rate of $5e-6$. A ReduceLROnPlateau scheduler based on validation loss was employed (factor=0.5, patience=5) to dynamically adjust the learning rate.

Evaluation Metrics. This study employs three metrics—Time-Adjacent Accuracy (TAA), Mean Squared Error (MSE), and Mean Absolute Error (MAE)—to comprehensively evaluate the predictive performance of the model. TAA is defined as the proportion of cases where the absolute deviation between the predicted recurrence or survival time and the true value does not exceed two years. This metric directly reflects the model's value in clinical decision support. These metrics together provide a comprehensive assessment of the model's prediction accuracy and stability.

$$TP - Acc = \frac{1}{N} \sum_{i=1}^N \mathbb{I}(|t_{pred}^{(i)} - t_{true}^{(i)}| \leq 2) \quad (7)$$

where $\mathbb{I}(\cdot)$ is the indicator function and N is the sample size.

4.3 Comparative Experiments

To validate the superiority of the proposed model (STG), we conducted a systematic comparison with existing methods, focusing on graph neural network architectures, feature extraction strategies, and multimodal fusion mechanisms. The results are presented in three subsections below.

Comparison of Graph Neural Network Backbone Architectures. We compared the performance of different graph neural network architectures, including Graph Convolutional Network (GCN), Graph Attention Network (GAT), and GraphSAGE (Table 2). The results show that GraphSAGE outperforms GCN and GAT in modeling multimodal heterogeneous graphs. In recurrence prediction, GraphSAGE achieves a TAA of 0.6667, outperforming GCN (0.4211) and GAT (0.3684) by 58.4% and 80.9%, respectively. Its MAE (1.6139) is also lower than GCN (2.3747) and GAT (2.5131), indicating its effective neighborhood sampling. In survival analysis, GraphSAGE leads with a TAA of 0.8462 and MAE of 1.1005, surpassing GCN (TAA=0.5789, MAE=1.8802) and GAT (TAA=0.6842, MAE=1.6727). These results highlight GraphSAGE’s advantages in handling modality differences and reducing redundant attention parameters.

Comparison of Feature Extraction Backbone Networks. In the image feature extraction module, we compared 3D ResNet18, R(2+1)D-18, and our custom-built shallow 3D convolutional network (with two convolution layers and a multi-scale pyramid pooling module trained on ImageNet). The results show in Table 3 that 3D ResNet18 is the most robust in a multitask scenario. In recurrence prediction, it outperforms both R(2+1)D-18 (MAE = 1.6366, TAA = 0.5641) and the custom-built model (MAE = 2.8758, TAA = 0.3590) with an MAE of 1.6139 and TAA of 0.6667. Although R(2+1)D-18 slightly outperforms 3D ResNet18 in survival analysis (MAE = 0.9957 vs. 1.1005), its limitations in recurrence prediction highlight that spatiotemporal decoupling convolution is insufficient for modeling static image features. Thus, 3D ResNet18 was chosen as the backbone network for multimodal joint optimization.

Table 2: Comparative Experiments for Graph Neural Network Backbone Architectures.

Model	Task	Metrics		
		TAA \uparrow	MSE \downarrow	MAE \downarrow
GCN	Recurrence	0.4211	7.4085	2.3747
	Survival	0.5789	4.6668	1.8802
GAT	Recurrence	0.3684	8.0947	2.5131
	Survival	0.6842	3.7087	1.6727
GraphSAGE	Recurrence	0.6667	3.7488	1.6139
	Survival	0.8462	1.7501	1.1005

Table 3: Comparative Experiments for Feature Extraction Backbone Networks.

Model	Task	Metrics		
		TAA \uparrow	MSE \downarrow	MAE \downarrow
Self-built model	Recurrence	0.3590	11.4129	2.8758
	Survival	0.4359	7.0232	2.3117
R(2+1)D-18	Recurrence	0.5641	3.7620	1.6366
	Survival	0.8462	1.5379	0.9957
3D ResNet18	Recurrence	0.6667	3.7488	1.6139
	Survival	0.8462	1.7501	1.1005

Comprehensive Comparison with Existing Models. To evaluate the proposed model (STG), we conducted a comparison (Table 4) with unimodal and traditional multimodal methods. The unimodal 3D ResNet18, using only preoperative CT image features, performs poorly in survival analysis (TAA = 0.1000, MAE = 82.3114) and recurrence prediction (MSE = 392.8506), showing that a single modality cannot capture tumor dynamics and its interaction with clinical indicators. Traditional multimodal methods show some improvement but still fall short. The early fusion method 3D-CNN achieves an MAE of 2.0250 in survival analysis, while late-stage feature concatenation with 3D-ResNet18 results in an MAE of 5.3590, due to their inability to model complex cross-modal relationships effectively. In contrast, STG improves cross-modal interaction through heterogeneous graph construction and spatiotemporal decoupling. In recurrence prediction, the TAA increases to 0.6667, and the MAE decreases to 1.6139. In survival analysis, the TAA reaches 0.8462, with an MAE of 1.1005, a 45.7% improvement over the best-performing multimodal baseline model (MAE = 2.0250).

Table 4: Comparative Experiments with Existing Models.

Types	Task	Metrics		
		TAA \uparrow	MSE \downarrow	MAE \downarrow
Single:3D ResNet18	Recurrence	0.3750	392.8506	53.6125
	Survival	0.1000	666.6192	82.3114
Multimodal:3 D-CNN	Recurrence	0.5250	6.6750	1.8750
	Survival	0.3750	5.6250	2.0250
Multimodal:3 D-ResNet18	Recurrence	0.6154	21.3333	3.1795
	Survival	0.2308	38.2308	5.3590
STG	Recurrence	0.6667	3.7488	1.6139
	Survival	0.8462	1.7501	1.1005

4.4 Ablation Studies

Our work presents three key innovations: the construction of multimodal heterogeneous graphs, a spatiotemporal graph reconstruction framework, and a spatiotemporal feature decoupling mechanism. To evaluate the contributions of each module, we incrementally introduce key components based on the 3D ResNet18 baseline model and assess their impact on recurrence prediction and survival analysis tasks. The baseline model performs direct regression by extracting CT image features using 3D ResNet18 without incorporating graph structures or multimodal fusion strategies. As shown in Table 5, the baseline model exhibits poor performance in recurrence prediction, with a Time-Aware Accuracy (TAA) of 0.3750, Mean Squared Error (MSE) of 392.8506, and Mean Absolute Error (MAE) of 53.6125. The survival analysis task yields a TAA as low as 0.1000, with MSE and MAE reaching 666.6192 and 82.3114, respectively. These results indicate that relying solely on static spatial features from imaging is inadequate for capturing the dynamic evolution of the tumor microenvironment and cross-modal associations, thus validating the necessity of spatiotemporal modeling and multimodal fusion.

By integrating a graph neural network (GNN) into the baseline model and constructing the spatial topological relationships between anatomical nodes, the model performance significantly improves. The MSE and MAE for recurrence prediction drop sharply to 16.4584 and 3.4640, respectively, while the TAA for survival analysis increases to 0.2105. This improvement confirms that the graph structure effectively models spatial heterogeneity between lesions, enhancing the discriminative power of feature representations. Upon further fusion of multimodal data, the synergy between clinical indicators and imaging features boosts the TAA for recurrence prediction to 0.5263, while survival analysis TAA reaches 0.8947, with MSE and MAE reduced to 2.2525 and 1.1983, respectively. These results suggest that the dynamic interaction of cross-modal edges significantly mitigates the limitations of single-modal information and fully unleashes the complementary value of imaging and clinical data.

Next, we introduce the spatiotemporal graph reconstruction framework, using GraphSAGE to reconstruct temporal graph sequences and aggregate spatiotemporal features. The model performance is further enhanced, with the recurrence prediction TAA increasing to 0.7895, and MSE and MAE for survival analysis dropping to 2.2868 and 1.1060, respectively. This outcome validates the effectiveness of temporal graph reconstruction for modeling dynamic prognostic patterns, enabling the simulation of long-term postoperative evolution. After employing the spatiotemporal feature decoupling mechanism, the model maintains excellent performance with a lightweight design, with the survival analysis TAA stabilizing at 0.8462 and MSE further reducing to 1.6203. This demonstrates that the decoupled spatiotemporal modeling strategy significantly improves computational efficiency and generalization ability by independently optimizing spatial topology and temporal dynamics, while reducing the model's parameter count.

Table 5: Different types of ablation experiments.

Types	Task	Metrics		
		TAA \uparrow	MSE \downarrow	MAE \downarrow
3Dresnet18	Recurrence	0.3750	392.8506	53.6125
(baseline)	Survival	0.1000	666.6192	82.3114
+ GNN	Recurrence	0.3684	16.4584	3.4640
	Survival	0.2105	15.5398	3.5020
+ Fusion	Recurrence	0.5263	4.2416	1.8593
	Survival	0.8947	2.2525	1.1983
+Reconstruction	Recurrence	0.7895	2.9332	1.5193
	Survival	0.8421	2.2868	1.1060
+ Spatiotemporal	Recurrence	0.5897	3.5424	1.5719
	Survival	0.8462	1.6203	1.0664
+ Contrastive	Recurrence	0.6667	3.7488	1.6139
	Survival	0.8462	1.7501	1.1005

The inclusion of contrastive learning enhances the model's robustness under data augmentation. With 20% node missing, the TAA for recurrence prediction remains stable at 0.6667, and the MAE for survival analysis only slightly increases to 1.1005. Contrastive learning reduces the impact of incomplete data by aligning feature spaces. The complete model, combining multimodal heterogeneous graph construction, spatiotemporal graph reconstruction, and lightweight decoupling mechanisms, achieves optimal performance in both recurrence prediction and survival analysis. The survival analysis TAA reaches 85%, with an MAE of 1.1005, outperforming existing methods. Experimental results show that the model's modules enable fine-grained tumor spatiotemporal modeling and meet lightweight deployment needs, providing reliable support for CRLM prognostic prediction.

5 Conclusion

This study addresses the clinical challenges of prognostic prediction for colorectal cancer liver metastasis (CRLM) by proposing an innovative framework that integrates a multimodal spatiotemporal graph neural network (STG). By constructing a heterogeneous graph structure from preoperative CT imaging lesions and clinical features, and applying GraphSAGE convolution along with LSTM decoupled spatiotemporal feature extraction, we have achieved a joint representation of tumor spatial heterogeneity and temporal evolution. Under a multi-task learning framework, the model simultaneously predicts recurrence risk and survival time, and utilizes contrastive learning to enhance feature fusion. Experimental results on a publicly available dataset demonstrate the effectiveness of our approach: compared to traditional methods and other deep models, our model

outperforms in both recurrence prediction and survival analysis metrics, showing strong potential for clinical application.

However, our study has some limitations. For instance, the evaluation metrics used are relatively few, and additional metrics could be incorporated for a more comprehensive assessment of the model's performance. Additionally, the temporal dimension in our model relies only on rough, discrete information from preoperative to postoperative follow-up; future work could explore incorporating finer-grained longitudinal data, such as imaging dynamic change curves. Moreover, integrating pathology, genetic, and other modalities into the graph model could further enhance the accuracy and robustness of predictions. In future work, we plan to collaborate with multiple centers to obtain more data to verify the model's generalization ability and explore the application of this method to metastasis prognostic prediction in other cancers. We believe that the multimodal spatiotemporal modeling approach based on graph neural networks holds great promise in the field of medical AI, providing a more reliable decision support tool for individualized cancer treatment.

REFERENCES

- [1] Birrer, D. L., Tschuor, C., Reiner, C. S., et al. (2021). Multimodal treatment strategies for colorectal liver metastases. *Swiss Medical Weekly*, 151, w20390. DOI: 10.4414/smw.2021.20390
- [2] Bray, F., Ferlay, J., Soerjomataram, I., et al. (2018). Global cancer statistics 2018: GLOBOCAN estimates of incidence and mortality worldwide for 36 cancers in 185 countries. *CA: A Cancer Journal for Clinicians*, 68(6), 394–424. DOI: 10.3322/caac.21492
- [3] Kokkinakis, S., Ziogas, I. A., Llaque Salazar, J. D., et al. (2024). Clinical prediction models for prognosis of colorectal liver metastases: a comprehensive review of regression-based and machine learning models. *Cancers (Basel)*, 16(9), 1645. DOI: 10.3390/cancers16091645
- [4] Kickingeder, P., Burth, S., Wick, A., et al. (2016). Radiomic profiling of glioblastoma: identifying an imaging predictor of patient survival with improved performance over clinical models. *Radiology*, 281(3), 907–918. DOI: 10.1148/radiol.2016160845
- [5] Topol, E. J. (2023). As artificial intelligence goes multimodal, medical applications multiply. *Science*, 381(6663), adk6139. DOI: 10.1126/science.adk6139
- [6] McKinney, S. M., Sieniek, M., Godbole, V., et al. (2020). International evaluation of an AI system for breast cancer screening. *Nature*, 577(7788), 89–94. DOI: 10.1038/s41586-019-1799-6
- [7] Zhou, S., Sun, D., Mao, W., et al. (2023). Deep radiomics-based fusion model for prediction of bevacizumab treatment response and outcome in patients with colorectal cancer liver metastases: a multicentre cohort study. *EClinicalMedicine*, 65, 102271. DOI: 10.1016/j.eclinm.2023.102271
- [8] Mobadersany, P., Yousefi, S., Amgad, M., et al. (2018). Predicting cancer outcomes from histology and genomics using convolutional networks. *Proceedings of the National Academy of Sciences*, 115(13), E2970–E2979. DOI: 10.1073/pnas.1717139115
- [9] Qu, Y., Zhai, X., Zhang, J., et al. (2023). Dynamic radiomics for predicting the efficacy of antiangiogenic therapy in colorectal liver metastases. *Frontiers in Oncology*, 13, 1106728. DOI: 10.3389/fonc.2023.1106728
- [10] Jin, C., Yu, H., Ke, J., et al. (2021). Predicting treatment response from longitudinal images using multi-task deep learning. *Nature Communications*, 12(1), 1851. DOI: 10.1038/s41467-021-22188-y
- [11] Gogoshin, G., & Rodin, A. S. (2023). Graph neural networks in cancer and oncology research: emerging and future trends. *Cancers (Basel)*, 15(24), 5858. DOI: 10.3390/cancers15245858
- [12] Andersen, P. K., & Gill, R. D. (1982). Cox's regression model for counting processes: a large sample study. *Annals of Statistics*, 10(4), 1100–1120. DOI: 10.1214/aos/1176345976
- [13] Liu, Y., Zhang, Y., Wang, J., et al. (2022). Deep learning from CT images for survival prediction in colorectal liver metastases. *European Radiology*, 32(5), 3421–3430. DOI: 10.1007/s00330-021-08444-1
- [14] Fong, Y., Fortner, J., Sun, R. L., et al. (1999). Clinical score for predicting recurrence after hepatic resection for metastatic colorectal cancer: analysis of 1001 consecutive cases. *Annals of Surgery*, 230(3), 309–321. DOI: 10.1097/0000658-199909000-00004
- [15] Fu, X., Patrick, E., Yang, J. Y. H., et al. (2023). Deep multimodal graph-based network for survival prediction from highly multiplexed images and patient variables. *Computerized Medical Imaging and Graphics*, 102, 102128. DOI: 10.1016/j.compmedimag.2023.102128
- [16] Wang, Z., Ma, J., Gao, Q., et al. (2024). Dual-stream multi-dependency graph neural network enables precise cancer survival analysis. *Medical Image Analysis*, 97, 103252. DOI: 10.1016/j.media.2024.103252
- [17] Yang, P., Chen, W., & Qiu, H. (2024). MMGCN: Multi-modal multi-view graph convolutional networks for cancer prognosis prediction. *Computer Methods and Programs in Biomedicine*, 257, 108400. DOI: 10.1016/j.cmpb.2024.108400
- [18] Yan, S., Xiong, Y., & Lin, D. (2018). Spatial temporal graph convolutional networks for skeleton-based action recognition. In *Proceedings of the IEEE Conference on Computer Vision and Pattern Recognition (CVPR)* (pp. 7444–7452). DOI: 10.1109/CVPR.2018.00776
- [19] Hao, Y., Wu, F., Zhou, J., et al. (2025). DSCASurv: Dual-stream cross-modal fusion alignment network for survival analysis with pathology images and genomics. *Briefings in Bioinformatics*, 26(2), bbad131. DOI: 10.1093/bib/bbad131
- [20] Hamilton, W. L., Ying, R., & Leskovec, J. (2017). Inductive representation learning on large graphs. In *Advances in Neural Information Processing Systems (NeurIPS)*, 30, 1025–1035.
- [21] Simpson, A. L., Peoples, J., Creasy, J. M., et al. (2024). Preoperative CT and survival data for patients undergoing resection of colorectal liver metastases. *Scientific Data*, 11(1), 172. DOI: 10.1038/s41597-024-02981-2